PLANT SCIENCE TODAY
ISSN 2348-1900 (online)
Vol x(x): xx–xx
https://doi.org/10.14719/pst.2489

HORIZON
e-Publishing Group

RESEARCH ARTICLE

Evaluating the Production Potential of Six *Combretum* Species in the Biomimetic Synthesis of Silver Nanoparticles

S N Egonu[1*], U C Okafor[1, 2], C C Isuosuo[1], O E Udoh[1], C K Chukwuemeka[1], E G Njoku[1] & O S Udengwu[1]

[1]Department of Plant Science and Biotechnology, University of Nigeria, Nsukka Campus, Enugu State-410001, Nigeria

[2]Department of Crop Sciences and Agroforestry, Faculty of Tropical Agrisciences, Czech University of Life Sciences, Prague, Kamycka 129, 165 000 Prague, Czech Republic

***Email:** sheily.egonu@unn.edu.ng

OPEN ACCESS

ARTICLE HISTORY
Received: 21 March 2023
Accepted: 29 June 2023
Available online
Version 1.0 : 11 January 2024

Check for updates

Additional information

Peer review: Publisher thanks Sectional Editor and the other anonymous reviewers for their contribution to the peer review of this work.

Reprints & permissions information is available at https://horizonepublishing.com/journals/index.php/PST/open_access_policy

Publisher's Note: Horizon e-Publishing Group remains neutral with regard to jurisdictional claims in published maps and institutional affiliations.

Indexing: Plant Science Today, published by Horizon e-Publishing Group, is covered by Scopus, Web of Science, BIOSIS Previews, Clarivate Analytics, NAAS,UGC Care etc. See https://horizonepublishing.com/journals/index.php/PST/indexing_abstracting

CITE THIS ARTICLE
Egonu S N, Okafor U C, Isuosuo C C, Udoh O E, Chukwuemeka C K, Njoku E G, Udengwu O S. Evaluating the Production Potential of Six Combretum Species in the Biomimetic Synthesis of Silver Nanoparticles. Plant Science Today (Early Access). https://doi.org/10.14719/pst.2489

Abstract

Existing research has shown that plants are best suited for the ecofriendly green synthesis of nanoparticles. This study presents novel findings on the biomimetic synthesis of silver nanoparticles using the aqueous leaf extract of six medicinal plant species in the genus, *Combretum* (*C. paniculatum, C. dolichopetalum, C. platypterum, C. racemosum, C. bauchiense,* and *C. demeusei*). The study focuses on conducting phytochemical screening of aqueous leaf extract, characterization, antimicrobial and cytological evaluation of the synthesized silver nanoparticles (AgNPs). The additional contribution of the study is the introduction of a nanoparticle production index (NPPI) of the species based on their crystalline sizes (in nm) and yield (in mg/l) of AgNPs. The NPPI represents a measure of the quantity of particles produced relative to the experimental species. The study aims to investigate whether these species, belonging to same genus yield similar results. The results indicate that smaller nanoparticle sizes correspond to higher production indices. Among the species, *C. paniculatum* demonstrated the highest production index (18.75 nm, 144.6 mg/l), while *C. demeusei* exhibited the lowest production index (0 nm, 6.3 mg/l). The AgNPs were characterized using various standard analytical techniques, including X-ray diffraction analysis which reveals 2 theta values in the 40° range, all corresponding to miller indices of (200). Furthermore, the synthesized AgNPs exhibited varying but significant antimicrobial activities, and the majority of the species showed a high NPPI. The study introduced the concept of "phytonanotaxonomy", which involves classifying plants of the same taxa based on their NPPI.

Keywords

Combretum; nanoparticle production index (nppi); biomimetic; phytonanotaxonomy; silver nanoparticles

Introduction

Particles that are extremely small, with at least one dimension under 100 nanometers (nm) are referred to as nanoparticles (NPs) (1). Noble metals such as silver (Ag), gold (Au), and copper (Cu) have nanoparticles that exhibit a broad absorption band in the visible region of the solar electromagnetic spectrum. In the field of modern material science, precise control over the synthesis of metal nanoparticles in terms of their facets, sizes, and shapes is of great importance (2).

Silver nanoparticles (AgNPs) have gained increasing attention due to their remarkable properties such as high conductivity, catalytic activity,

localized surface plasmon resonance, antibacterial capabilities, and chemical durability (3). Among various metal nanoparticles, AgNPs have emerged as particularly promising materials. They find applications in diverse fields, including targeted medication delivery, as antimicrobials (4), anti-cancer medicines (5-7), biosensors (8), and pest management in agriculture (9).

Due to the drawbacks of chemico-physical procedures, such as the use of toxic chemicals, high temperatures, pressure, and the formation of hazardous by-products, it is essential to explore safer alternative methods for the production of AgNPs. In this regard, the biological synthesis of nanoparticles using microorganisms such as bacteria, fungi, algae, and plant extracts has gained increasing importance (10,11). These biological approaches offer several advantages over chemical and physical processes as they don't require high temperatures or pressure and provide non-toxic, more economical, and ecologically friendly alternatives (12). Moreover, studies have demonstrated that plant-mediated synthesis can yield a higher quantity of AgNPs **(**13, 14). These methods, commonly referred to as 'green synthesis', utilize plant extracts and microorganisms to mimic chemical processes in an eco-friendly manner, a concept known as biomimicry.

Among the 370 species in the Genus *Combretum*, approximately 300 are native to tropical and southern Africa. These plants have been long utilized in local traditional medicine across Africa and Asia for the treatment of various ailments. Despite the abundance of *Combretum* species, there is a scarcity of research on nanoparticle synthesis involving these plants, highlighting the need for further investigation. This study aims to expand the existing knowledge on *Combretum*-synthesized AgNP, specifically focusing on their antimicrobial and cytotoxic properties, their potential as high-yielding AgNP species, and to provide a valuable academic resource for students and researchers involved in future studies on *Combretum* species.

To the best of our knowledge, this study represents the first documentation of the synthesis of AgNPs using the aqueous leaf extract of six *Combretum* species: *C. paniculatum*, *C. dolichopetalum*, *C. platypterum, C. racemosum, C. bauchiense,* and *C. demeusei*. The major objectives of this study were to quantitatively analyze the phytochemical composition of the leaf extracts to identify the biomolecules responsible for the synthesis and stabilization of AgNPs. Additionally, the synthesized nanoparticles were characterized using various analytical techniques. Furthermore, an NPPI (NanoParticle Production Index) was created based on the size and yield of nanoparticle produced by each species. The antimicrobial activities of the synthesized nanoparticles against bacterial and fungal pathogens were evaluated, and cytological effect of AgNPs on the root tips of *Allium sativum* (garlic) was examined to assess possible chromosomal aberrations.

Materials and Methods

Collection of Plants and Preparation of Leaf Extracts

Fresh leaves of *C. paniculatum*, *C. dolichopetalum*, *C. platypterum, C. racemosum, C. bauchiense,* and *C. demeusei* were collected from Nsukka (Enugu State – Nigeria) metropolis. The leaves were thoroughly washed with running water and then dried in the lab (shade dry). On completely dry, the plants were ground into a fine powder. Twenty grams of each powder was weighed and transferred into separate 500 ml Erlenmeyer flask. To each flask, 400 ml of distilled water was added, and the mixture was boiled for 20 minutes in a water bath set at 80 °C. After boiling, the mixtures were allowed to cool at room temperature. Subsequently, the mixture in each flask was first filtered using cheesecloth and then with Whatman No.1 filters paper. The resulting filtrate (extract) was collected and used for the synthesis process.

Synthesis of Silver Nanoparticles

For the synthesis, 10 ml of each plant extract was added to 90ml of a 3mM $AgNO_3$ solution. The reaction mixture was then placed in a dark cupboard and monitored for visible color change. The samples were observed for a period of 48h before proceeding for characterization.

NanoParticle Production Index (NPPI)

The NPPI for the synthesized AgNPs from the study plants was determined by evaluating the crystalline sizes of the synthesized AgNPs and measuring the yield of AgNPs in mg/l (using a Mettler Toledo sensitive balance) after centrifugation and lyophilization of the reaction mixture.

Characterization of the Synthesized Nanoparticles

The absorption spectra of the AgNPs were obtained using a UV spectrophotometer (UV-1800 Shimadzu), followed by centrifugation and lyophilization. The morphologies of the particles were determined using scanning electron microscopy (SEM) with a Phenom ProX instrument. The crystalline nature and size of the AgNPs were analyzed using an X-ray diffractometer (XRD) with a Rigaku MiniFlex300. Fourier transform infrared spectroscopy (FTIR) was performed using a Cary 630 instrument, and dynamic light scattering (DLS) was carried out using a Zetasizer Nano ZS

Phytochemical Analysis

The plant extracts underwent quantitative phytochemical screening to determine the presence of various phytochemicals, including tannins, flavonoids, oxalate, phenolics, saponin and alkaloids, among others. The procedures conducted were in accordance with the official analytical methods (15).

Antimicrobial Activity Assay (Antibacterial and Antifungal)

A total of six pathogens were used for the study, including two Gram-negative bacteria (*P. aeruginosa* and *E. coli*), two Gram-positive bacteria (*B. cereus* and *S. aureus*) and two fungi (*A. flavus* and *A. niger*). The assay was conducted by modifying the agar well diffusion assay described by (16). Aliquots of 60 µl of each plant-AgNPs, at varying

concentrations (25 mg/ml, 12.5 mg/ml, 6.25 mg/ml, 3.125 mg/ml and 1.56 mg/ml), were added to pre-formed wells in the culture plates that were already seeded with the test organisms. The plates (bacterial) were then incubated at 37 °C for 18 – 24 hrs and plates (fungal) at 25 – 27 °C for 48 h respectively. The antimicrobial activity of each plant mediated AgNPs was determined by measuring the zone of inhibition (ZOI) surrounding each well. A stock solution of 3 mM $AgNO_3$ and the plant extracts were used as positive controls.

Cytological Study using Allium Test

Garlic" bulbs (*A. sativum*) were used as the testing material in the *Allium* test with modifications based on (17). Two concentration of each plant-AgNP -solution, a low concentration (0.5mg) and a high concentration (1.0mg) were used. The root tips of the garlic bulbs were exposed to the different concentrations of the plant-AgNP solution for different time periods (24 and 48hrs). Root tips left in distilled water only served as the negative control, providing a baseline for comparison to assess the effects of the tested materials. After treatment, the roots tips were cut off and prepared for slide examination using a Philip Harris light microscope equipped with a Moticam Image Plus 2.0 camera. Each slide contained two root tips, which were observed to evaluate the effects of AgNPs on the chromosomes during the different stages of mitosis and to detect any chromosomal aberrations resulting from the action of the particles.

Result and Discussion

Visual Examination of Synthesis and UV-visible Spectroscopy

When the plant extracts (10ml) were added to 3mM of $AgNO_3$ (90ml), the solution exhibited an immediate change in the color, which deepened over time in all cases (0 – 48 hrs). The color transformation observed were as follows: *C. paniculatum* AgNPs changed from red to deep red; *C. dolichopetalum* AgNPs changed from light brown to dark brown; *C. platypterum* AgNPs changed from yellowish to reddish orange; *C. racemosum* AgNPs, changed from brownish to dark brown; *C. bauchiense* AgNPs changed from reddish to deep brown, and *C. demeusei* AgNPs changed from yellow to reddish (Fig 1 and 2). The corresponding reduced AgNPs exhibited distinct visible absorption peaks at wavelengths of 442.07, 440.06, 447, 461.05, 433.91 and 430.14 nm respectively (Figures 3A – 3F). The color change observed in the original plant extract/$AgNO_3$ solution mixture is an initial indication of affirmative nanoparticle synthesis. These changes, which are confirmed by UV-vis spectroscopy, demonstrated characteristic absorption peaks, associated with surface plasmon resonance (SPR) of the AgNPs. AgNPs have the ability to absorb and scatter light due to the oscillations of free electrons on silver surface undergoing SPR when excited by light at specific wavelengths (18).

NanoParticle Production Index (NPPI)

Table 1 presents the nanoparticle production index (NPPI) for six *Combretum* species used in this study. The index was developed based on the crystalline sizes of the synthesized AgNPs and their yield in mg/l, where the species with smaller sizes and higher yield were assigned higher indices. From the table, it can be observed that *C. paniculatum* had the highest production index as it exhibited the smallest size (18.75nm) and the highest yield (144.6mg/l). Conversely, *C. demeusei* had the lowest index, as no crystalline size could be determined, and the yield was very low (6.3mg/l). The consistency of this pattern among the studied species was challenged only by the size -yield indices for *C. dolichopetalum,* which may be due to significant differences in values for atomic concentration of silver, Z average and soluble carbohydrate content compared to other species. Additionally, the darker coloured AgNP solutions obtained 48h after synthesis were consistent with higher yields as observed in the case of *C. paniculatum, C. dolichopetalum, C. racemosum* and *C. bauchiense.* However, *C. platypterum* and *C. demeusei*

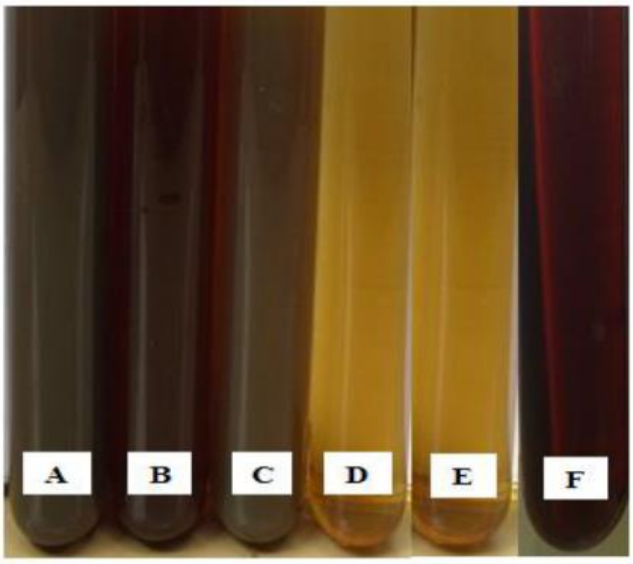

A- *C. dolichopetalum* AgNP solution, **B**- *C. bauchiense* AgNP solution, **C**- *C. racemosum* AgNP solution, **D**- *C. platypterum* AgNP solution, **E**- *C. demeusei* AgNP solution, **F**- *C. paniculatum* AgNP solution (0 hrs after synthesis)

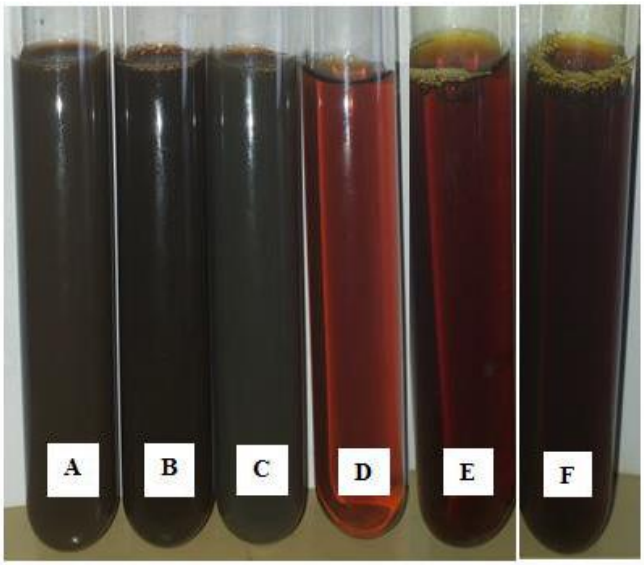

A- *C. dolichopetalum* AgNP solution, **B**- *C. bauchiense* AgNP solution, **C**- *C. racemosum* AgNP solution, **D**- *C. platypterum* AgNP solution, **E**- *C. demeusei* AgNP solution, **F**- *C. paniculatum* AgNP solution (48 hrs after synthesis)

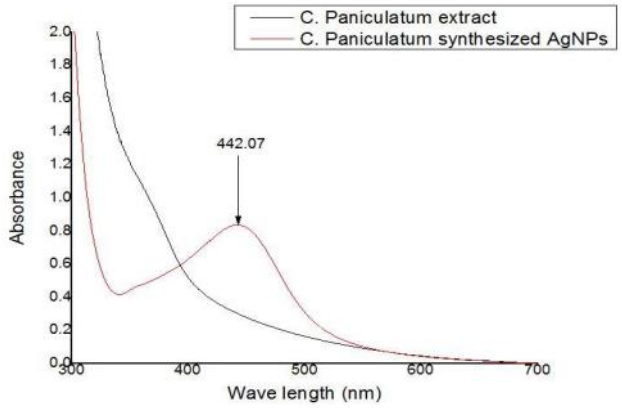

Fig. 3A. UV-vis Absorption Spectra of *C. paniculatum* AgNPs.

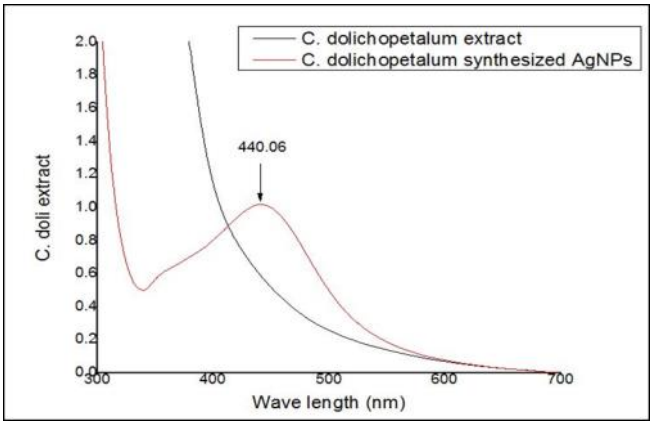

Fig. 3B. UV-vis Absorption Spectra of *C. dolichopetalum* AgNPs.

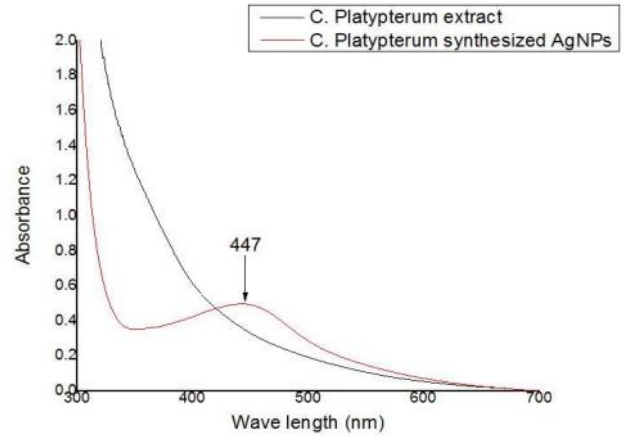

Fig. 3C. UV-vis Absorption Spectra of *C. platypterum* AgNPs.

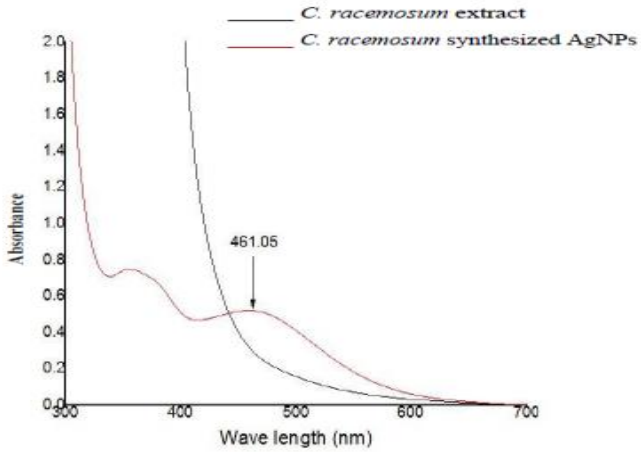

Fig. 3D. UV-vis Absorption Spectra of *C. racemosum* AgNPs.

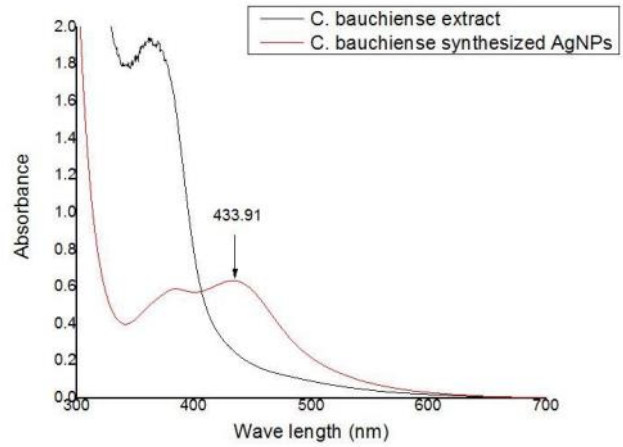

Fig. 3E. UV-vis Absorption Spectra of *C. bauchiense* AgNPs

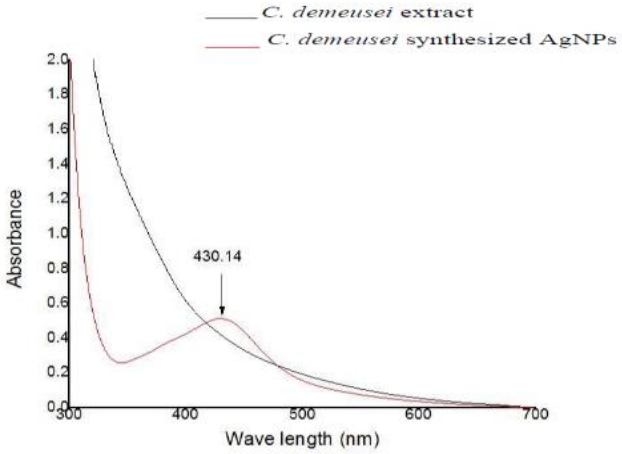

Fig. 3F. UV-vis Absorption Spectra of *C. demeusei* AgNPs.

exhibited color changes but remained lightly colored after the designated time period indicating low AgNP yield (Fig 1 and 2). While there is lack of Literature on experimental studies that quantifying the yield of silver nanoparticles after synthesis, the color patterns and the "Nanoparticle Production Index (NPPI)" established through synthesis, centrifugation and lyophilization strongly support the findings of (19), who noted that the color properties of AgNPs correlate with the number density of the nanoparticles. Thus, the NPPI can be described as a measure of the quantity of particles produced in relation to the experimental species used in the synthesis.

Table 1. Nano Particle Production Index (NPPI) showing AgNP yield and size indices

Species	AgNP size from XRD (nm)	Observed AgNP Yield in mg/l
C. paniculatum	18.75	144.6
C. dolichopetalum	37.88	113.7
C. bauchiense	18.98	105.8
C. racemosum	22.76	101.5
C. platypterum	-	9.2
C. demeusei	-	

SEM/SEM-EDX Characterization

The SEM micrographs in figures 4A – 4F depicts the morphology (shape) of the nanoparticles. The analysis indicates that the AgNPs exhibited different shapes across all species. In the *C. bauchiense* micrograph (figure 4E), the visible AgNPs appeared rounded, flat and even amorphous. Similarly, the *C. paniculatum* micrograph (figure 4A) also revealed AgNPs of various shapes. Just like physical and chemical routes of synthesis, plant mediated synthesis is capable of producing AgNPs of different shapes, which can be useful for various relevant applications (20-23).

It has been reported (24) that obtained AgNPs of varying shapes from a single plant is a common phenomenon when synthesizing particles using plant extracts. The shapes observed in this study are consistent with experiments conducted within the Combretaceae family (25 – 29).

The elemental analysis of the plant-mediated AgNPs produced in the study is presented in figures 5A – 5F. Each figure includes a key indicating the elements present and their percentage atomic concentration. SEM-EDX analysis provides insights into the elemental composition of the AgNPs. The peaks observed represents the positions assigned to the different elements, and the area under the peaks signifies the number of atoms of the corresponding elements present in the X-ray irradiated area of the samples, as indicated in the accompanying key for each case. The distinctiveness of EDX spectroscopy in elemental composition detection stems from the unique atomic structure of each element, which generates characteristics peak on an electromagnetic spectrum (30, 31). The elements identified in the AgNPs synthesized in the study align with finding from other investigations on

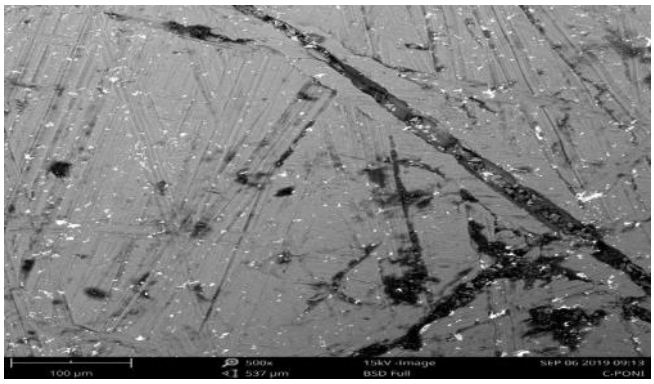

Fig. 4A. SEM micrograph showing *C. paniculatum* AgNPs.

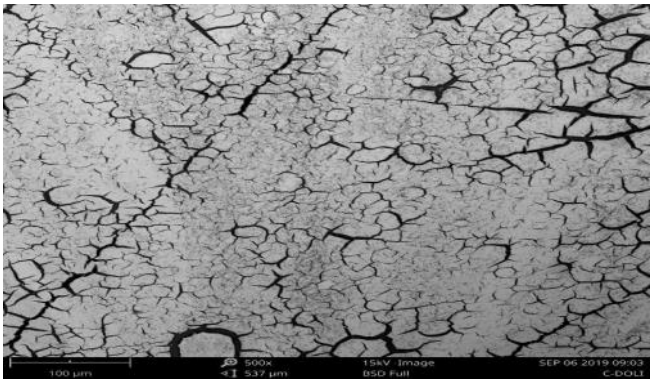

Fig. 4B. SEM micrograph showing *C. dolichopetalum* AgNPs.

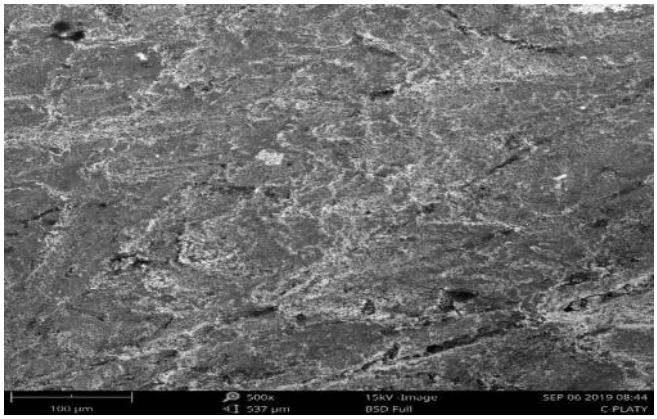

Fig. 4C. SEM micrograph showing *C. platypterum* AgNPs.

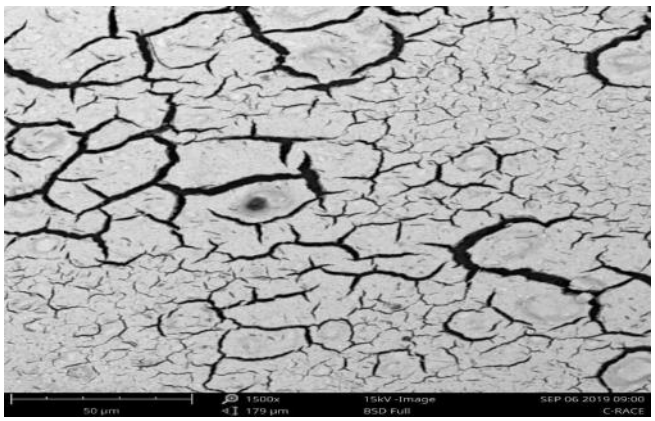

Fig. 4D. SEM micrograph showing *C. racemosum*- AgNPs.

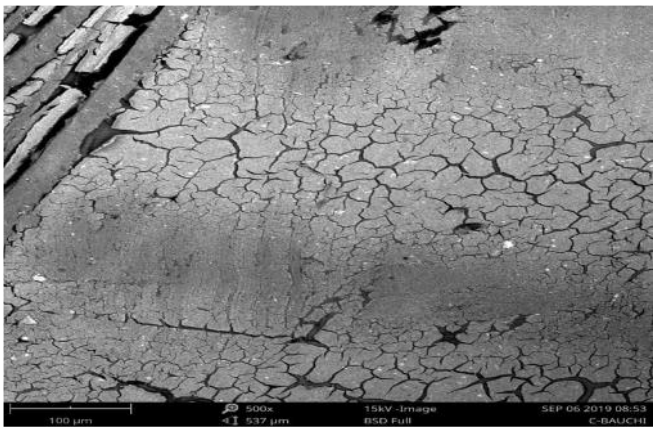

Fig. 4E. SEM micrograph showing *C. bauchiense*- AgNPs.

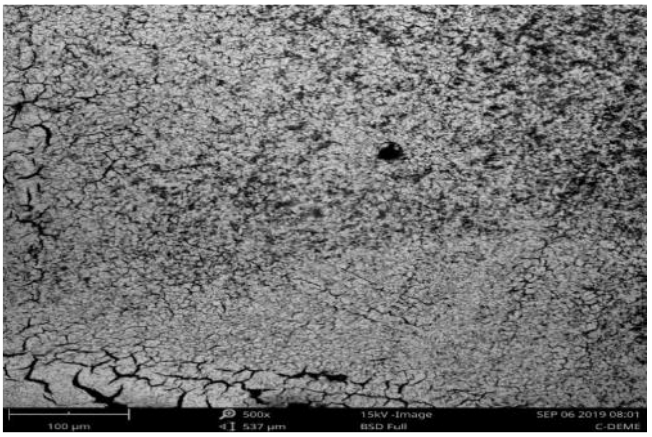

Fig. 4F. SEM micrograph showing *C. demeusei*- AgNPs.

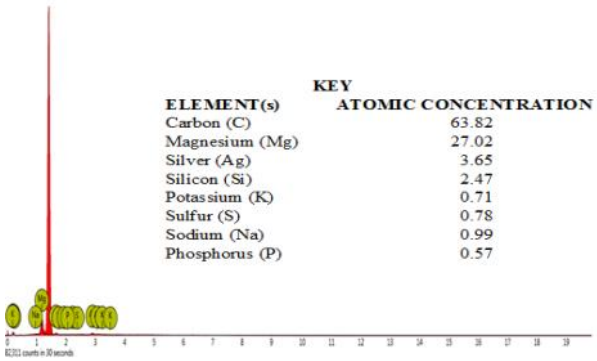

Fig. 5A. SEM-EDX representation of elements present in *C. paniculatum* AgNPs.

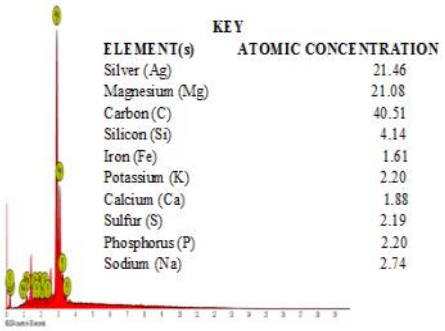

Fig. 5B. SEM-EDX representation of elements present in *C. dolichopetalum* AgNPs.

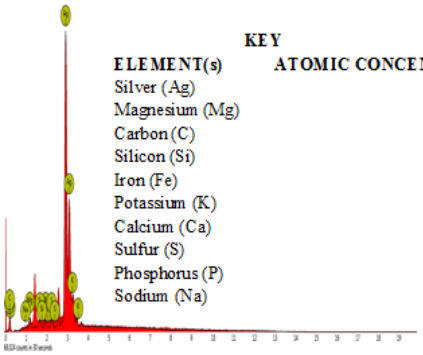

Fig. 5C. SEM-EDX representation of elements present in *C. platypterum* AgNPs.

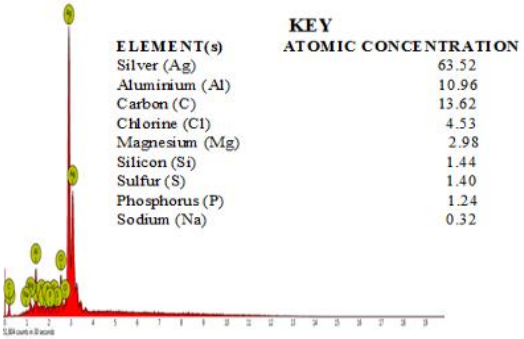

Fig. 5D. SEM-EDX representation of elements present in *C. racemosum* AgNPs.

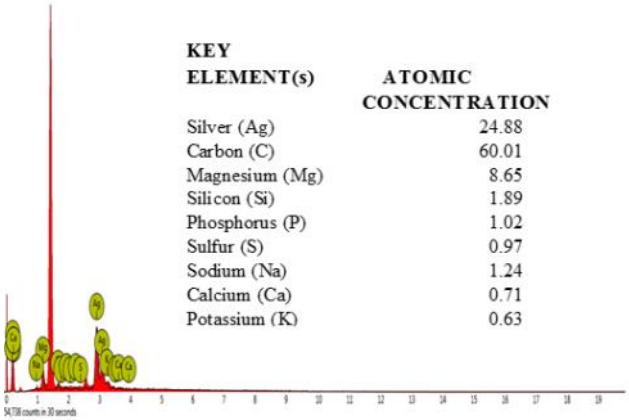

Fig. 5E. SEM-EDX representation of elements present in *C. bauchiense* AgNPs.

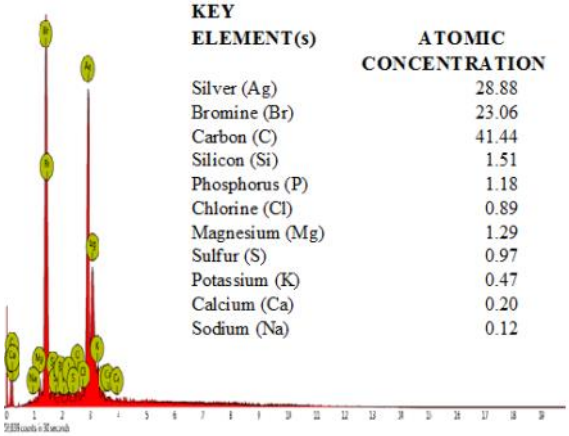

Fig. 5F. SEM-EDX representation of elements present in *C. demeusei* AgNPs.

Combretum species (29).

Characterization by X-ray Diffraction (XRD)

XRD is an analytical technique that provides insights into the crystalline nature of the synthesized AgNPs and can also be used to determine their crystalline size.The diffractograms shown in figures 6A – 6F exhibit distinct diffraction peaks. Braggs reflections observed at 2 theta angle values of 44.08°, 41.01°, 44.36° and 44.42° were obtained for *C. dolichopetalum*, *C. paniculatum, C. bauchiense* and *C. racemosum* AgNPs, respectively. These reflections corresponded to hkl miller index of (200) in all cases. The average crystalline sizes were calculated using the Debye-Scherrer's formula and were found to be 37.88 nm, 18.75nm, 18.98nm and 22.76nm, respectively. However, the diffractogram of Ag nanoparticles synthesized with *C. demeusei* showed no peaks corresponding to Ag nanoparticles. Similarly, for *C. platypterum*, the broad peak observed at 21.23° may be attributed to the leaf extract used for the synthesis. It is characteristic of AgNPs (and other nanoparticles) to have their atoms arranged into crystalline structures, which can be validated through XRD analysis by observing characteristic peaks and Miller indices. The XRD peaks at 2 theta are indexed to different crystallographic planes of Bragg's reflections and indicate whether the nanoparticles possess a face-centered cubic structure (FCC) or body-centered cubic (BCC) structure, thereby confirming their crystalline nature. The absence of peaks corresponding to silver in certain cases suggests that, during the reduction process, the atoms remained arranged in a more random fashion, exhibiting a greater level of amorphousness compared to crystalline structures, as only crystals yield

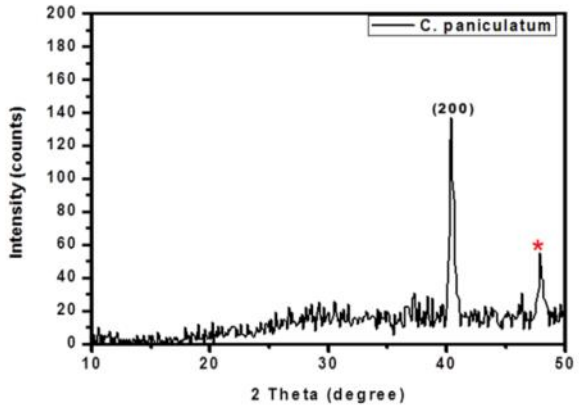

Fig. 6A. XRD pattern of *C. paniculatum* AgNPs.

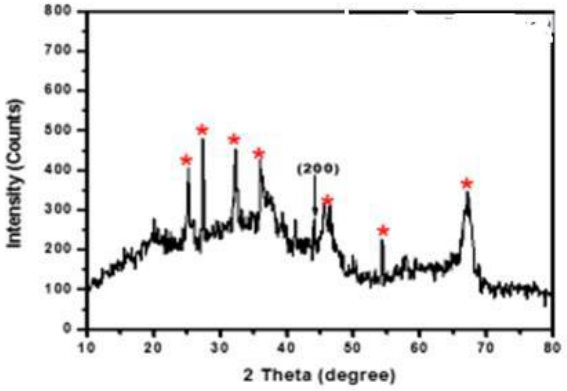

Fig. 6B. XRD pattern of *C. dolichopetalum* AgNPs.

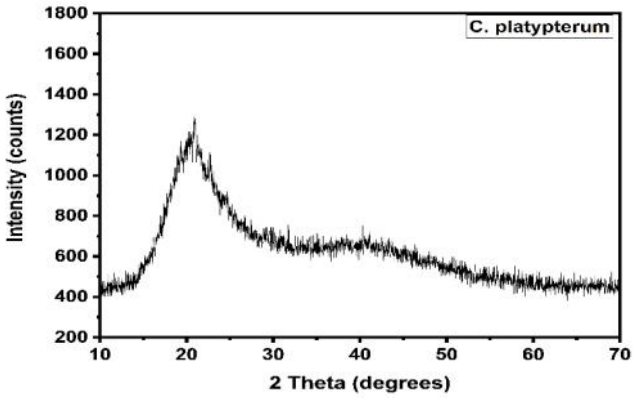

Fig. 6C. XRD pattern of *C. platypterum* AgNPs.

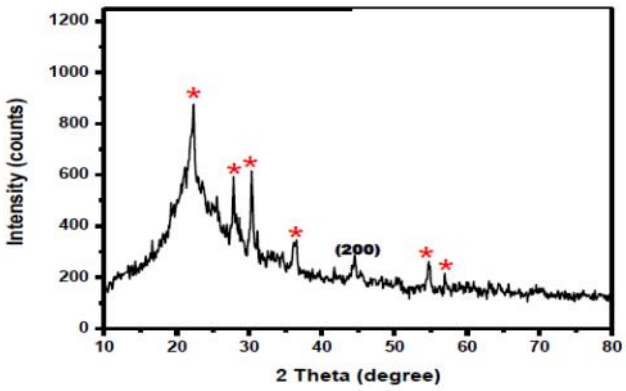

Fig. 6D. XRD pattern of *C. racemosum* AgNPs.

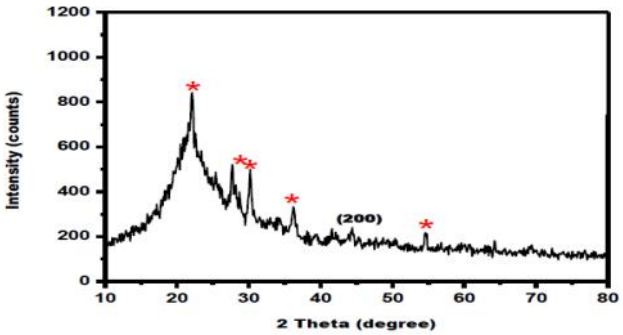

Fig. 6E. XRD pattern of *C. bauchiense* AgNPs.

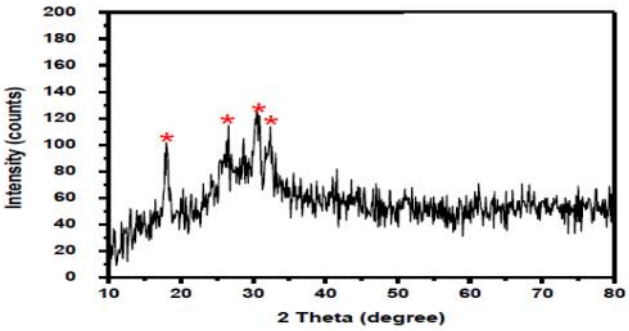

Fig. 6F. XRD pattern of *C. demeusei* AgNPs.

sharp peaks. The unassigned peaks, marked with asterisk are believed to arise due to the presence of phytochemical compounds in the leaf extract (32, 33).

DLS Characterization

The size distribution by intensity of the *Combretum*-synthesized AgNPs is presented in figures 7A – 7F. The scatter of the size distribution graph indicates the average size (Z average) of the AgNPs, with a broader scatter suggesting smaller average size and a narrower scatter suggesting larger average size of the AgNPs. Figure 7A illustrates the size distribution of *C. paniculatum* AgNPs, showing a broad scatter and Z average size of 289 nm. Figure 7B depicts the size distribution of *C. dolichopetalum* AgNPs, also exhibiting a broad scatter with a Z average size 131.3nm. Figure 7E represents the size distribution of *C. bauchiense* AgNP, which displays two peaks. The major peak exhibits a narrow scatter, indicating a larger Z average size of 757.8nm. For *C. racemosum* AgNPs shown in figure 7D, three peaks are observed. The major peak demonstrates a narrow scatter and Z average size is 567.2 nm. Figure 7C represents the size distribution of *C. platypterum* AgNPs, showing a narrow scatter and a Z average size of 240.7 nm. Finally, figure 7F displays the size distribution of *C. demeusei* AgNPs, with the major peak exhibiting a narrow scatter and a Z average of 90.75nm. The Polydispersity Index (PDI) values for *C. paniculatum* AgNPs, *C. dolichopetalum* AgNPs, *C. bauchiense* AgNPs and *C. racemosum* AgNPs were 0.4, 0.4, 0.6 and 0.6 respectively. *C. platypterum* AgNPs had a PDI of 0.4, while *C. demeusei* AgNPs had a PDI of 0.3. Dynamic light scattering (DLS) offers numerous advantages as an analytical technique and provides the insights into the behavior of nanoparticles in a solution system. The Z-average, PDI (polydispersity index) and Zeta potential serve as “quality control” of the DLS technique. Polydispersity refers to the degree of non-uniformity of a size distribution of particles, whereby the lower the PDI value, the closer it is to achieving a monodispersed system (34). Values less than 0.7 indicate stability whereas particles with PDI larger than 0.7 suggests broad particle size distribution (35-36).

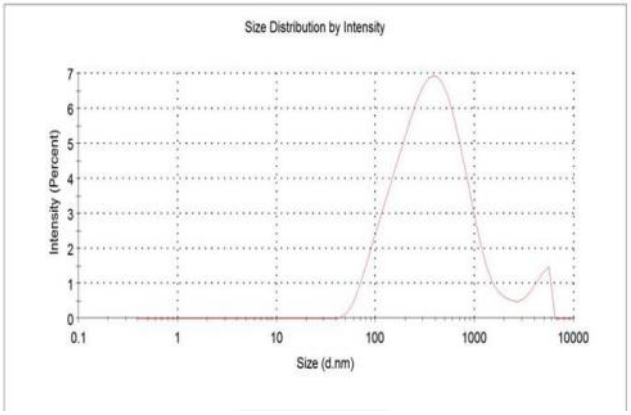

Fig. 7A. Size distribution by intensity of *C. paniculatum* AgNPs.

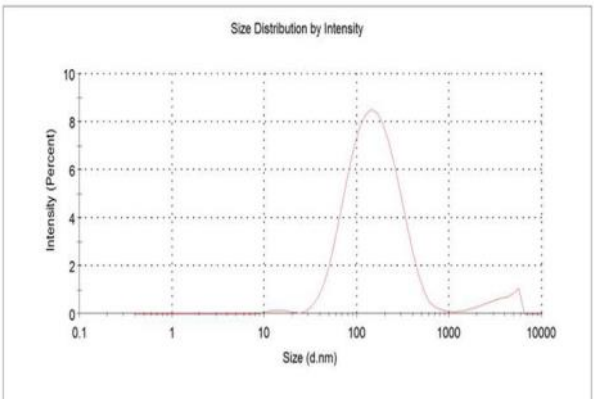

Fig. 7B Size distribution by intensity of *C. dolichopetalum* AgNPs.

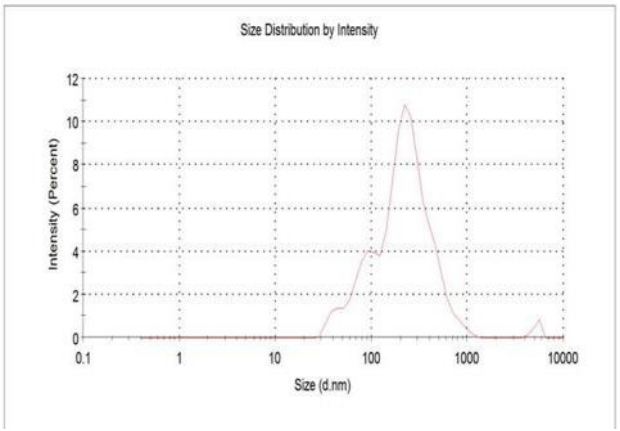

Fig. 7C. Size distribution by intensity of *C. platypterum* AgNPs.

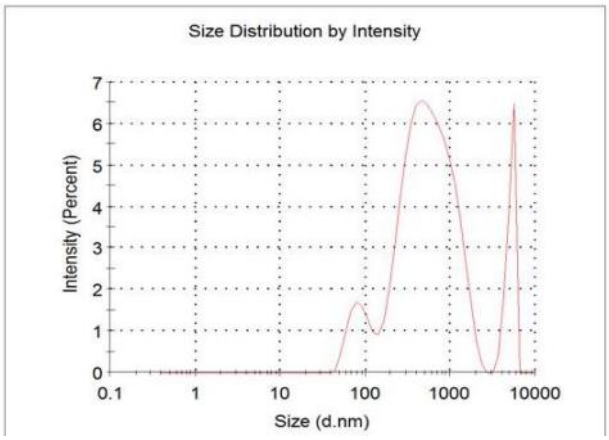

Fig. 7D. Size distribution by intensity of *C. racemosum* AgNPs.

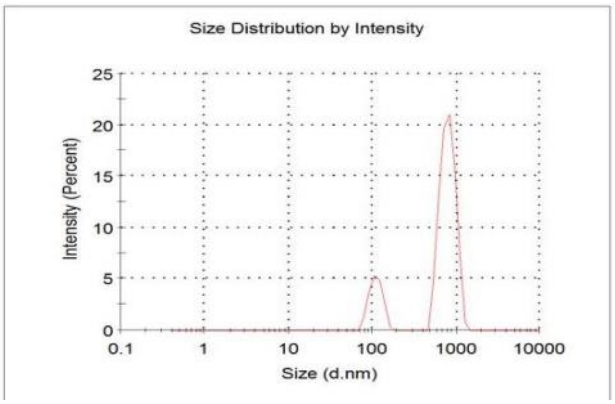

Fig. 7E. Size distribution by intensity of *C. bauchiense* AgNPs.

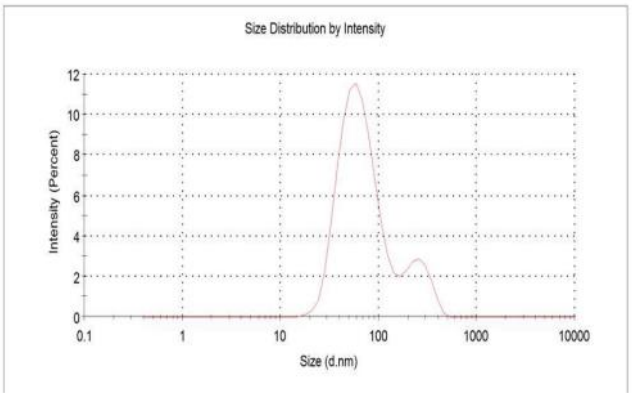

Fig. 7F. Size distribution by intensity of *C. demeusei* AgNPs.

Fourier Transform Infrared (FTIR) Spectroscopy Analysis

FTIR spectra obtained for the leaf extracts and silver nanoparticles synthesized using the leaf extracts are shown in figures 8A – 8F. The most prevalent functional groups across all the studied plants were amide, amine, O-H hydroxyl, and alkene. The FTIR spectra of silver nanoparticles, gives information about the local molecular environment of the organic molecules on the surface of the samples. The purpose of this analysis is to identify the biomolecules present which are potentially responsible for reduction of bulk silver to silver nanoparticles, as well as efficient stabilization of the formed silver nanoparticles. According to (37), these biomolecules contain bond linkages and functional groups that play active role in the synthesis process. The decreases in the number of peaks present in the plant extract when compared to the spectra of the AgNPs can be attributed to interactions between functional groups and the silver ions (38). The presence of O-H hydroxyl functional group, observed across all *Combretum* species in the study, is characteristic of polyphenols. Among the polyphenols, flavonoids are well-known for their ability to act as reducing agents during synthesis of AgNPs (39, 40).

Phytochemical Analysis

The results of the quantitative phytochemical analysis are presented in table 2. The distribution of phytochemicals varied significantly among all the studied plants. However, the highest values were consistently recorded for phenolics and flavonoids. The phytochemical analysis conducted in this study revealed high levels of flavonoids, which is in line with previous reports indicating that *Combretum* species are rich in polyphenols (41 – 43).

Table 2. Quantitative Phytochemical Analysis of Leaves of Study Plants (in mg/100ml)

Treatments	Phenolics	Tannins	Flavonoids	HCN	Red. Sugars	Steroids	Saponins	Sol. Carb	Terpenoids	Alkaloids
C. platypterum	43.04± 0.01^{c}	2.54 ± 0.00^{d}	46.97 ± 0.01^{d}	0.006 ± 0.00^{c}	20.11 ± 0.00^{d}	0.01 ± 0.00^{e}	0.13 ± 0.00^{d}	2.20 ± 0.00^{e}	0.79 ± 0.00^{a}	9.44 ± 0.06^{e}
C. dolichopetalum	14.31± 0.01^{e}	2.83 ± 0.01^{a}	79.47 ± 0.01^{b}	0.008 ± 0.00^{ab}	22.08 ± 0.01^{b}	0.03 ± 0.00^{c}	0.20 ± 0.00^{b}	18.06± 0.01^{a}	0.03 ± 0.00^{e}	9.73 ± 0.02^{c}
C. bauchiense	1.94 ± 0.01^{f}	2.67 ± 0.01^{b}	15.55 ± 0.00^{f}	0.007 ± 0.00^{bc}	20.73 ± 0.00^{c}	0.15 ± 0.00^{a}	0.20 ± 0.00^{b}	0.46 ± 0.00^{f}	0.11 ± 0.00^{d}	9.86 ± 0.00^{b}
C. paniculatum	54.85 ± 0.00^{b}	1.90 ± 0.00^{e}	72.68 ± 0.00^{c}	0.002 ± 0.00^{d}	1.74 ± 0.00^{e}	0.02 ± 0.00^{d}	0.17 ± 0.00^{c}	4.60 ± 0.01^{d}	0.49 ± 0.00^{b}	10.29± 0.01^{a}
C. demeusei	42.94 ± 0.01^{d}	1.43 ± 0.00^{f}	26.17 ± 0.00^{e}	0.001 ± 0.00^{e}	28.06 ± 0.01^{a}	0.00± 0.00^{f}	0.12 ± 0.00^{e}	5.18 ± 0.00^{b}	0.33 ± 0.00^{c}	5.18 ± 0.05^{f}
C. racemosum	56.99 ± 0.01^{a}	2.61 ± 0.01^{c}	148.27 ± 0.01^{a}	0.008 ± 0.00^{a}	28.06 ± 0.00^{a}	0.10 ± 0.00^{b}	0.32 ± 0.00^{a}	4.86 ± 0.00^{c}	0.11± 0.00^{d}	9.71 ± 0.00^{d}

Mean value with different alphabet in each column are significantly different from each other by DMRT (P≤0.05)

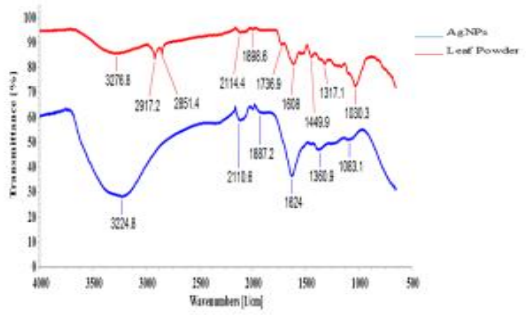

Fig. 8A. FTIR spectra showing peaks representing various functional groups present in *C. paniculatum* AgNPs and *C. paniculatum* leaf powder.

Fig. 8B. FTIR spectra showing peaks representing various functional groups present in *C. dolichopetalum* AgNPs and *C. dolichopetalum* leaf powder.

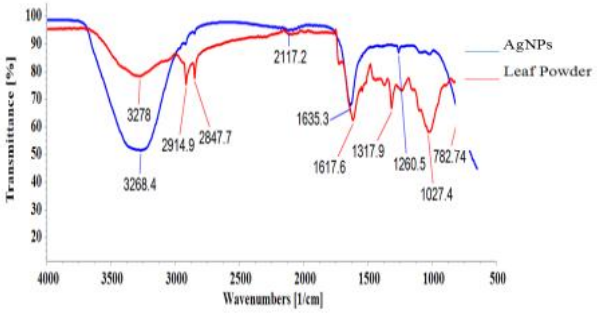

Fig. 8C. FTIR spectra showing peaks representing various functional groups present in *C. platypterum* AgNPs and *C. platypterum* leaf powder.

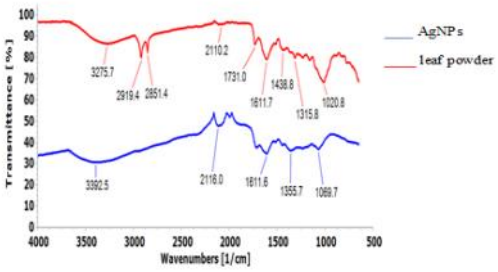

Fig. 8D. FTIR spectra showing peaks representing various functional groups present in *C. racemosum* AgNPs and *C. racemosum* leaf powder.

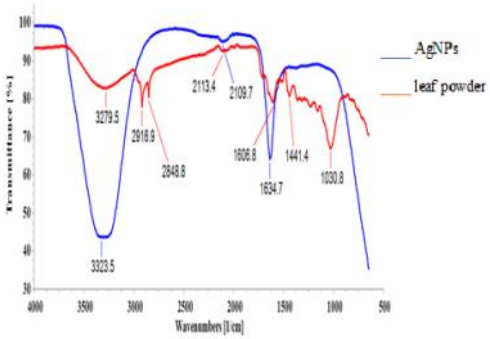

Fig. 8E. FTIR spectra showing peaks representing various functional groups present in *C. bauchiense* AgNPs and *C. bauchiense* leaf powder.

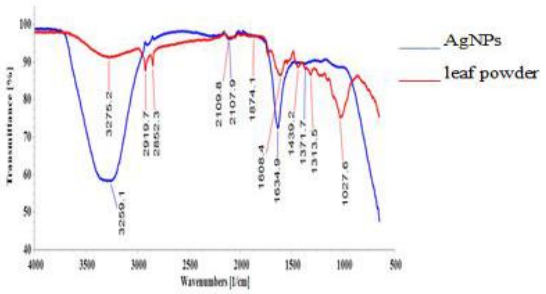

Fig. 8F. FTIR spectra showing peaks representing various functional groups present in *C. demeusei* AgNPs and *C. demeusei* leaf powder.

Antimicrobial Activity

The antimicrobial activity assay was carried out to evaluate the potential of the synthesized AgNPs to inhibit the growth of the aforementioned test organisms. Clear zones of inhibition (ZOI) indicated by red arrows in figures 9A – 9C, and were observed. Figure 9A shows the susceptibility of *B. cereus* while Figure 9B demonstrates the susceptibility of *A. flavus* to *C. paniculatum* AgNPs. Additionally, Figure 9C demonstrates susceptibility of *A. flavus* to *C. racemosum* AgNPs.

Table 3 presents the mean Zone of Inhibition (ZOI) diameter of the different plant-mediated AgNPs at various concentrations, against the Gram positive bacteria; *Bacillus cereus* and *Staphylococcus aureus*. The *C. dolichopetalum* AgNPs exhibited significant inhibition against *S. aureus* and *P. aeruginosa* across all tested concentrations. However, *C. bauchiense* AgNPs showed no inhibition against both test organisms. *C. racemosum* AgNPs exhibited inhibition against *B. cereus* at all test concentrations, while susceptibility of *S. aureus* was only at the highest test concentration (25 mg/ml). *C. paniculatum* AgNPs on the other hand exhibited significant inhibition against *B. cereus* at all tested concentrations, while inhibition against *S. aureus* was observed only at concentration of 12.5 mg/ml. On the other hand, no inhibition was observed by *C. platypterum* and *C. demeusei* AgNPs against both test organisms. It is also noteworthy that the plant extracts of *C. racemosum* and *C. bauchiense*, which served as controls, showed minimal inhibition against *S. aureus*. Bulk silver ($AgNO_3$) also showed varying levels of inhibition.

Table 4 represents the mean Zone of Inhibition (ZOI) diameter of the different plant- mediated AgNPs at various concentrations, against the Gram negative bacteria; *Escherichia coli* and *Pseudomonas aeruginosa*. *C. dolichopetalum* AgNPs exhibited significant inhibition against *P. aeruginosa* across all tested concentrations. However, no inhibition was observed against *E. coli*. *C. bauchiense* AgNPs exhibited inhibition against *E. coli* at all tested concentrations, while minimal susceptibility was observed against *P. aeruginosa* at the highest concentration tested (25 mg/ml). *C. racemosum* AgNPs inhibited the growth of *E. coli* only at a concentration of 25 mg/ml, while inhibition against *P. aeruginosa* was observed across all tested concentrations. *C. platypterum* AgNPs inhibited the growth of *P. aeruginosa* at concentrations of 25 mg/ml and 12.5 mg/ml, but no inhibition was observed against *E. coli*. *C. demeusei* AgNPs exhibited inhibition against *E. coli* only at a concentration of 25 mg/ml. In the case of *C. paniculatum* AgNPs, significant inhibition was observed against both organisms. It is noteworthy that the inhibition was more

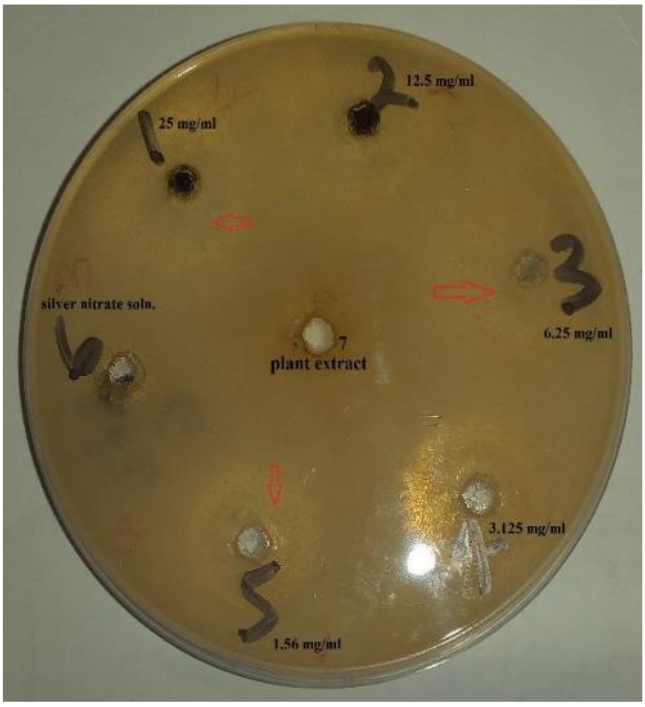

Fig. 9B. showing effect of *C. paniculatum* AgNPs on *A. flavus.*

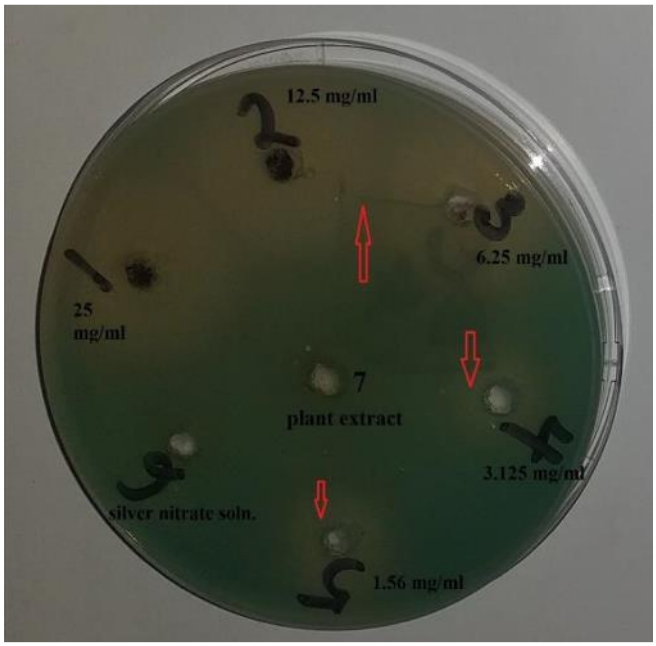

Fig. 9A. showing effect of *C paniculatum* AgNPs on *B. cereus.*

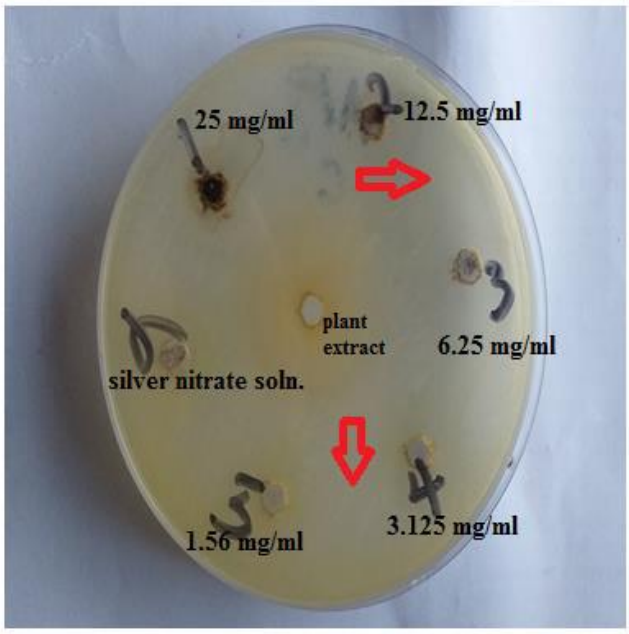

Fig. 9C. showing effect of *C. racemosum* AgNPs on *A. flavus.*

pronounced at the higher concentrations tested (6.25 mg/ml, 12.5 mg/ml, and 25 mg/ml).

Table 3. Antibacterial Activity of AgNPs against Gram Positive Bacteria

Plant-AgNPs	Concentration	*B. cereus* Mean ZOI of AgNPs (mm)	*S. aureus*
C. dolichopetalum	25 mg/ml	14.66±1.20^{a2}	8.00±4.04^{b2}
	12.5 mg/ml	12.33±0.88^{a2,3}	10.66±1.31^{b1}
	6.25 mg/ml	14.00±1.52^{a2}	8.66±1.33^{b2}
	3.125 mg/ml	8.66±1.52^{3}	7.66±0.65^{2}
	1.56 mg/ml	12.66±2.06^{a2}	7.33±0.35^{b2,3}
	Control ($AgNO_{3)}$	18.66±1.52^{a1}	10.55±1.03^{b1}
	Control (Plant Extract)	0.00±0.00^{4}	0.00±0.00^{4}
C. bauchiense	25 mg/ml	0.00±0.00^{2}	0.00±0.00^{3}
	12.5 mg/ml	0.00±0.00^{2}	0.00±0.00^{3}
	6.25 mg/ml	0.00±0.00^{2}	0.00±0.00^{3}
	3.125 mg/ml	0.00±0.00^{2}	0.00±0.00^{3}
	1.56 mg/ml	0.00±0.00^{2}	0.00±0.00^{3}
	Control ($AgNO_3$)	9.00±1.00^{b1}	11.00±4.00^{a1}
	Control (Plant Extract)	0.00±0.00^{b2}	5.66±0.81^{a2}
C. racemosum	25 mg/ml	14.33±3.05^{a2}	9.00±2.81^{b1}
	12.5 mg/ml	4.33±0.78^{a4}	0.00±0.00^{b3}
	6.25 mg/ml	6.00±1.29^{a3}	0.00±0.00^{b3}
	3.125 mg/ml	6.00±0.79^{a3}	0.00±0.00^{b3}
	1.56 mg/ml	0.00±0.00^{5}	0.00±0.00^{3}
	Control ($AgNO_3$)	19.33±4.04^{a1}	10.55±0.95^{b1}
	Control (Plant Extract)	0.00±0.00^{b5}	5.00±5.00^{a2}
C. platypterum	25 mg/ml	0.00±0.00^{2}	0.00±0.00^{2}
	12.5 mg/ml	0.00±0.00^{2}	0.00±0.00^{2}
	6.25 mg/ml	0.00±0.00^{2}	0.00±0.00^{2}
	3.125 mg/ml	0.00±0.00^{2}	0.00±0.00^{2}
	1.56 mg/ml	0.00±0.00^{2}	0.00±0.00^{2}
	Control ($AgNO_3$)	19.00±4.35^{a1}	6.33±0.96^{b1}
	Control (Plant Extract)	0.00±0.00^{2}	0.00±0.00^{2}
C. demeusei	25 mg/ml	0.00±0.00^{2}	0.00±0.00^{2}
	12.5 mg/ml	0.00±0.00^{2}	0.00±0.00^{2}
	6.25 mg/ml	0.00±0.00^{2}	0.00±0.00^{2}
	3.125 mg/ml	0.00±0.00^{2}	0.00±0.00^{2}
	1.56 mg/ml	0.00±0.00^{2}	0.00±0.00^{2}
	Control ($AgNO_3$)	12.00±1.00^{1}	11.66±1.77^{1}
	Control (Plant Extract)	0.00±0.00^{2}	0.00±0.00^{2}
C. paniculatum	25 mg/ml	29.00±3.60^{a1}	0.00±0.00^{b2}
	12.5 mg/ml	23.33±2.11^{a2}	15.66±4.04^{b1}
	6.25 mg/ml	23.33±1.23^{a2}	0.00±0.00^{b2}
	3.125 mg/ml	17.00±2.00^{a3}	0.00±0.00^{b2}
	1.56 mg/ml	16.00±2.00^{a3}	0.00±0.00^{b2}
	Control ($AgNO_3$)	18.66±5.85^{a3}	0.00±0.00^{b2}
	Control (Plant Extract)	0.00±0.00^{4}	0.00±0.00^{2}

Data are presented with means ± standard error, significance (P≤0.05) was separated using Duncan Multiple Range Test (DMRT). Means bearing same alphabets and numbers are not significant whereas those with different numbers and alphabets are significant

Table 4. Antibacterial Activity of AgNPs against Gram Negative Bacteria

Plant-AgNPs	Concentration	*E. coli* Mean ZOI of AgNPs (mm)	*P. aeruginosa*
C. dolichopetalum	25 mg/ml	0.00±0. 00^{b}	16.00±1.00^{a1}
	12.5 mg/ml	0.00±0.00^{b}	12.66±1.52^{a2}
	6.25 mg/ml	0.00±0.00^{b}	12.00±0.00^{a2}
	3.125 mg/ml	0.00±0.00^{b}	12.00±0.00^{a2}
	1.56 mg/ml	0.00±0.00^{b}	11.00±0.00^{a2}
	Control ($AgNO_{3)}$	0.00±0.00^{b}	12.00±1.00^{a2}
	Control (Plant Extract)	0.00±0.00	0.00±0.003
C. bauchiense	25 mg/ml	8.0±2.00^{a1}	0.57±0.33^{b2}
	12.5 mg/ml	2.66±0.61^{a3}	0.00±0.00^{b3}
	6.25 mg/ml	6.66±1.54^{a2}	0.00±0.00^{b3}
	3.125 mg/ml	7.66±0.27^{a1}	0.00±0.00^{b3}
	1.56 mg/ml	8.33±1.43^{a1}	0.00±0.00^{b3}
	Control ($AgNO_3$)	4.00±0.92^{b2,3}	18.33±2.08^{a1}
	Control (Plant Extract)	5.00±0.66^{a2}	0.00±0.00^{b3}
C. racemosum	25 mg/ml	7.33±0.42^{b1}	13.33±3.05^{a3}
	12.5 mg/ml	0.00±0.00^{b2}	13.66±1.52^{a3}
	6.25 mg/ml	0.00±0.00^{b2}	14.00±2.00^{a2}
	3.125 mg/ml	0.00±0.00^{b2}	14.00±2.00^{a2}
	1.56 mg/ml	0.00±0.00^{b2}	16.66±3.51^{a1,2}
	Control ($AgNO_3$)	0.00±0.00^{b2}	18.00±0.00^{a1}
	Control (Plant Extract)	0.00±0.00^{2}	0.00±0.004
C. platypterum	25 mg/ml	0.00±0.00^{b2}	10.33±3.05^{a2}
	12.5 mg/ml	0.00±0.00b^{2}	9.33±1.52^{a2}
	6.25 mg/ml	0.00±0.00^{2}	0.00±0.00^{3}
	3.125 mg/ml	0.00±0.00^{2}	0.00±0.00^{3}
	1.56 mg/ml	0.00±0.00^{2}	0.00±0.00^{3}
	Control ($AgNO_3$)	14.66±4.16^{b1}	19.00±2.00^{a1}
	Control (Plant Extract)	0.00±0.00^{2}	0.00±0.00^{3}
C. demeusei	25 mg/ml	2.66±0.61^{a2}	0.00±0.00^{b2}
	12.5 mg/ml	0.00±0.00^{3}	0.00±0.00^{2}
	6.25 mg/ml	0.00±0.00^{3}	0.00±0.00^{2}
	3.125 mg/ml	0.00±0.00^{3}	0.00±0.00^{2}
	1.56 mg/ml	0.00±0.00^{3}	0.00±0.00^{2}
	Control ($AgNO_3$)	6.66±1.52^{a1}	2.33±1.52^{b1}
	Control (Plant Extract)	0.00±0.00^{3}	0.00±0.00^{2}
C. paniculatum	25 mg/ml	16.00±2.64^{b1}	18.00±2.64^{a2}
	12.5 mg/ml	15.33±1.20^{1,2}	15.66±1.50^{3}
	6.25 mg/ml	13.00±0.56^{3}	14.00±2.11^{3}
	3.125 mg/ml	0.00±0.00^{4}	0.00±0.00^{4}
	1.56 mg/ml	0.00±0.00^{4}	0.00±0.00^{4}
	Control ($AgNO_3$)	17.33±3.78^{b1}	21.66±3.05^{a1}
	Control (Plant Extract)	0.00±0.004	0.00±0.004

Data are presented with means ± standard error, significance (P≤0.05) was separated using Duncan Multiple Range Test (DMRT). Means bearing same alphabets and numbers are not significant whereas those with different numbers and alphabets are significant

Table 5 presents the mean Zone of Inhibition (ZOI) diameters of different plant-mediated AgNPs at various concentrations against the fungi, *Aspergillus flavus* and *A. niger*. *C. dolichopetalum* AgNPs exhibited significant inhibition against *A. flavus*, except at a concentration of 6.25mg/ml, while no inhibition was observed in the case of *A. niger*. It is also worth noting that *C. dolichopetalum* plant extract showed minimal inhibition of the growth of *A. flavus*. *C. bauchiense* AgNPs inhibited the growth of *A. flavus* at a concentration of 25mg/ml, however, no inhibition was observed against *A. niger*. *A. flavus* showed susceptibility to *C. racemosum* AgNPs across all tested concentrations, while the susceptibility of *A. niger* was observed only at a concentration of 25mg/ml. *C. racemosum* plant extract also exhibited inhibition of growth in both test organisms. *C. platypterum* AgNPs inhibited the growth of A. flavus at a concentration of 25 mg/ml, and its plant extract showed minimal inhibition of the growth of *A. niger*. Both test organisms showed susceptibility to *C. demeusei* AgNPs at the highest tested concentration (25mg/ml). Lastly, *C. paniculatum* AgNPs

Table 5. Antifungal Activity of AgNPs

Plant/AgNPs	Concentration	*A. flavus* Mean ZOI of AgNPs (mm)	*A. niger*
C. dolichopetalum	25 mg/ml	$14.00\pm0.57^{a,1}$	0.00 ± 0.00^{b2}
	12.5 mg/ml	$12.66\pm2.08^{a,1}$	0.00 ± 0.00^{b2}
	6.25 mg/ml	0.00 ± 0.00^{4}	0.00 ± 0.00^{2}-
	3.125 mg/ml	$11.66\pm1.52^{a1,2}$	0.00 ± 0.00^{b2}
	1.56 mg/ml	12.00 ± 1.44^{a1}	0.00 ± 0.00^{b2}
	Control ($AgNO_3$)	13.00 ± 1.35^{a1}	2.66 ± 0.61^{b1}
	Control (Plant Extract)	4.33 ± 0.50^{a3}	0.00 ± 0.00^{b2}
C. bauchiense	25 mg/ml	11.00 ± 2.64^{a2}	0.00 ± 0.00^{b}
	12.5 mg/ml	0.00 ± 0.00^{3}	0.00±0.00
	6.25 mg/ml	0.00 ± 0.00^{3}	0.00±0.00
	3.125 mg/ml	0.00 ± 0.00^{3}	0.00±0.00
	1.56 mg/ml	0.00 ± 0.00^{3}	0.00 ± 0.00^{a}
	Control($AgNO_3$)	$16.00\pm3.60^{a,1}$	0.00 ± 0.00^{b}
	Control (Plant Extract)	0.00 ± 0.00^{3}	0.00±0.00
C. racemosum	25 mg/ml	13.33 ± 1.15^{a2}	7.66 ± 0.65^{b1}
	12.5 mg/ml	13.00 ± 2.30^{a2}	0.00 ± 0.00^{b2}
	6.25 mg/ml	13.66 ± 2.30^{a2}	0.00 ± 0.00^{b2}
	3.125 mg/ml	15.00 ± 2.00^{a1}	0.00 ± 0.00^{b2}
	1.56 mg/ml	8.00 ± 1.00^{a3}	0.00 ± 0.00^{b2}
	Control ($AgNO_3$)	15.33 ± 1.14^{a1}	0.00 ± 0.00^{b2}
	Control(Plant Extract)	5.00 ± 0.66^{b4}	7.33 ± 0.35^{a1}
C. platypterum	25 mg/ml	7.66 ± 0.65^{a2}	0.00 ± 0.00^{b2}
	12.5 mg/ml	0.00 ± 0.00^{3}	0.00 ± 0.00^{2}
	6.25 mg/ml	0.00 ± 0.00^{3}	0.00 ± 0.00^{2}
	3.125 mg/ml	0.00 ± 0.00^{3}	0.00 ± 0.00^{2}
	1.56 mg/ml	0.00 ± 0.00^{3}	0.00 ± 0.00^{2}
	Control ($AgNO_3$)	11.33 ± 1.86^{a1}	0.00 ± 0.00^{b2}
	Control(Plant Extract)	0.00 ± 0.00^{b3}	4.00 ± 0.92^{a1}
C. demeusei	25 mg/ml	2.66 ± 0.61^{a2}	3.00 ± 0.19^{a2}
	12.5 mg/ml	0.00 ± 0.00^{3}	0.00 ± 0.00^{3}
	6.25 mg/ml	0.00 ± 0.00^{3}	0.00 ± 0.00^{3}
	3.125 mg/ml	0.00 ± 0.00^{3}	0.00 ± 0.00^{3}
	1.56 mg/ml	0.00 ± 0.00^{3}	0.00 ± 0.00^{3}
	Control ($AgNO_3$)	15.00 ± 2.29^{a1}	11.66 ± 3.21^{b1}
	Control (Plant Extract)	0.00 ± 0.00^{3}	0.00 ± 0.00^{3}
C. paniculatum	25 mg/ml	27.33 ± 2.51^{a1}	0.00 ± 0.00^{b2}
	12.5 mg/ml	28.33 ± 2.08^{a1}	0.00 ± 0.00^{b2}
	6.25 mg/ml	27.33 ± 2.51^{a1}	0.00 ± 0.00^{b2}
	3.125 mg/ml	22.00 ± 1.73^{a2}	0.00 ± 0.00^{b2}
	1.56 mg/ml	20.00 ± 1.00^{a2}	0.00 ± 0.00^{b2}
	Control ($AgNO_3$)	$15.00\pm4.35^{-}$	11.33 ± 1.52^{b1}
	Control (Plant Extract)	0.00 ± 0.00^{4}	0.00 ± 0.00^{2}

Data are presented with means ± standard error, significance (P≤0.05) was separated using Duncan Multiple Range Test (DMRT). Means bearing same alphabets and numbers are not significant whereas those with different numbers and alphabets are significant

exhibited significant inhibition against *A. flavus* across all tested concentrations, while no inhibition was observed against *A. niger*.

The observed trend in the antimicrobial activity of the AgNPs indicates that inhibition increased in a dose-dependent manner. Additionally, minimal inhibition was observed at the higher concentrations tested. Various factors and mechanisms have been attributed to the effect of AgNPs on microorganisms. This study suggests that the differences in AgNP action may be associated with the yields of AgNPs, as reflected in the NPPI created. Species with higher production indices exhibited greater inhibitory activity against susceptible microorganisms compared to those with lower yields. Concentration-dependency is another factor to consider, as most of the AgNPs with minimal activity exhibited their effects at the highest concentrations tested. Moreover, the Zone of Inhibition (ZOI) increased in a concentration-dependent manner. These findings align with previous studies that have reported concentration-dependency as a factor influencing the activity of plant-mediated AgNPs (44 – 46).

Cytological Study using Allium test (Allium sativum)

Cytotoxicity studies serve as an important initial assessment to evaluate the potential harm that a test substance may cause. Cytotoxicity refers to the extent to which an agent can specifically damage certain cells. Assessing the effects of compounds or substances on cells is widely employed as an indicator of potential toxic effects (47).

Allium sativum, commonly known as garlic, is a well-established plant model system used for toxicity assessment. Among the various plant organs, root tips are particularly important as they are the first organs to come into direct contact with nanoparticles (NPs), making them a valuable basis for evaluating cytological alterations. The *Allium sativum* root assay offers several advantages, including its low cost, rapid root elongation activity, and the ability to distinguish different cell cycle phases. Moreover, it allows for the evaluation of a commonly measured endpoint: chromosomal aberrations (48). For these reasons, the *A. sativum* root assay has been widely utilized to assess chromosomal aberrations induced by various NPs, including AgNPs, as demonstrated in this study

The results of the *Allium* test conducted using the root tips of *Allium sativum* bulbs treated with different concentrations of the plant-synthesized AgNPs used in the study are presented in figures 10A – C. Figure 10A shows the occurrence of disturbed metaphase chromosomal aberration during mitosis in root tips treated with 1.0mg of *C. platypterum* AgNPs for 48h. In figure 10B, the presence of binucleate cells, indicated by a white arrow, can be observed in root tips treated with 0.5mg of *C. dolichopetalum* AgNPs for 24h. A normal uninucleate cell is indicated by a yellow arrow. Furthermore, figure 10C illustrates the occurrence of anaphase bridge aberration in root tips treated with 1.0mg of *C. racemosum* AgNPs for 24h (Fig.10C).

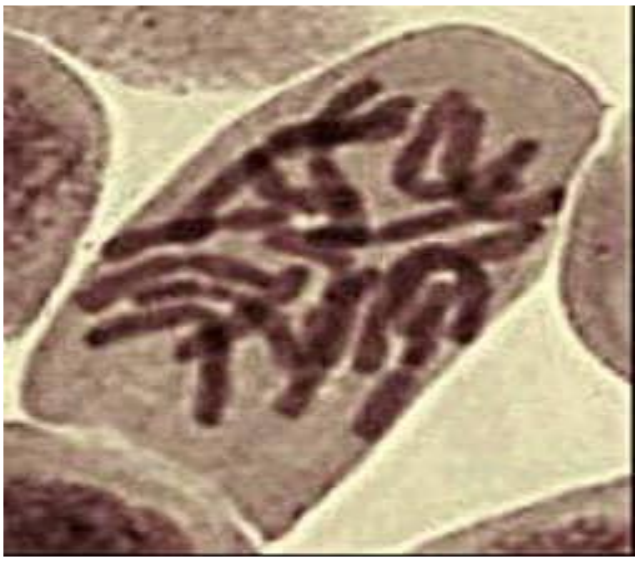

Figure. 10A. Disturbed metaphase chromosomal aberration observed during mitosis in the root tips of *Allium sativum* treated with 1.0mg *C. platypterum* AgNPs for 48h- (Magnification X400).

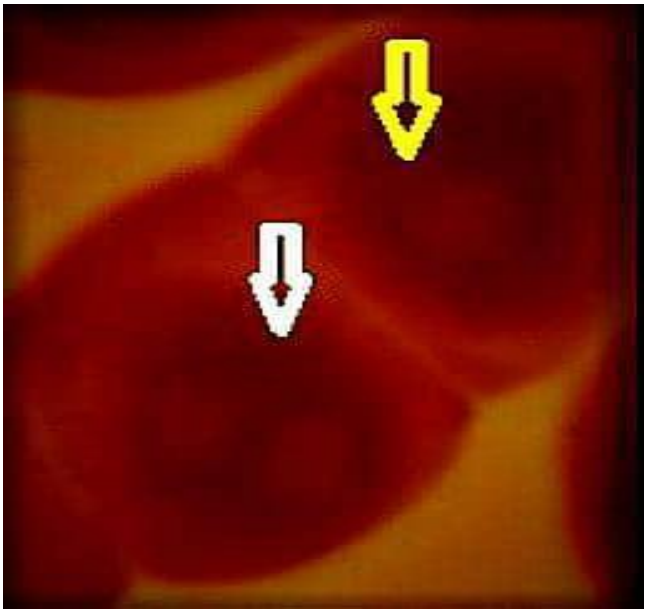

Figure. 10B. Binucleate cell chromosomal aberration observed during mitosis in the root tips of *Allium sativum* treated with 0.5 mg *C. dolichopetalum* AgNPs for 24h- (Magnification X400)

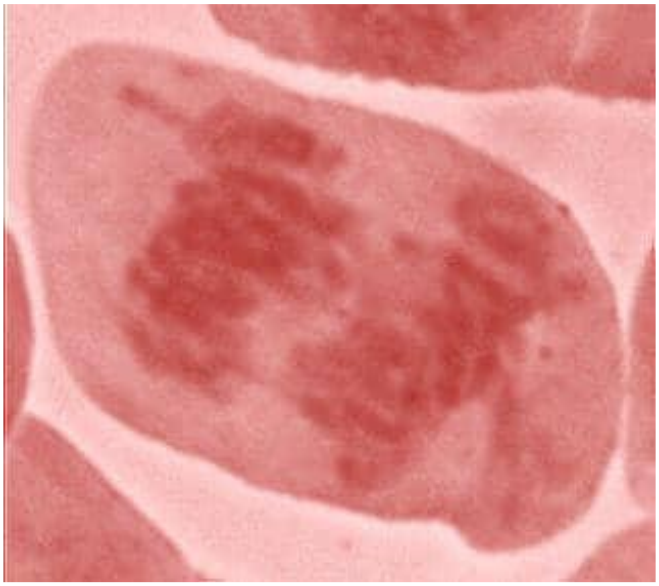

Figure. 10C. Anaphase bridge aberration observed during mitosis in the root tips of *Allium sativum* treated with 1.0mg *C. racemosum* AgNPs- for 24h (Magnification X400).

Table 6 provides a detailed description of the chromosomal aberrations observed in the Allium test. It is noteworthy that chromosomal aberrations were observed in both the control group and the treated root tips, except for the root tips treated with *C. bauchiense* AgNPs. However, the frequency of aberrations was higher in the treated groups compared to the control group.

In the standard Allium- test using *Allium sativum*, various morphological changes were observed in the chromosomes of the root tips treated with the AgNPs. Regardless of the test concentrations and exposure time, chromosomal aberrations were observed, including disturbed metaphase, binucleate cells and anaphase bridges. The occurrence of chromosomal bridges could be attributed to the breakage and fusion of chromosomes and chromatids, as well as terminal deletion or loss of telomeres(49). Disturbed metaphase, observed as changes during metaphase, may result from the effects of the particles on the mitotic spindle, altering their orientation. This impairment could be due to interactions of AgNPs with tubulin-SH. The formation of binucleate cells, resulting from the inhibition of cell-plates formation by AgNPs, indicates a failure to follow the normal mitotic process during cytokinesis. These binucleate cells have the potential to enter the next round of the cell cycle (50).

It is worth noting that like the chromosomal aberrations were also observed in control group of the Allium test, similar to previous report. Many experiments have reported the presence of chromosomal aberrations both in their controls groups and in treatment groups. Interestingly, these aberrations in controls may be as a result of environmental stress experienced by the cells or by the presence of free radicals. (51) reported that under certain conditions, plant products themselves can bring about mutagenic effects in the presence of multiple biological factors. Perhaps, these factors contribute to the occurrence of aberration observed in the “control” root tips. Therefore, the treatments in this study cannot be solely held accountable as the cause of the aberrations since same occurred in the control group.

While these chromosomal aberrations suggests that the AgNPs may have phytotoxic clastogenic and aneugenic effects to the plant, it is essential to consider various other factors such as the size, concentration and surface coating of the AgNPs, as well as the species, tissue and developmental stage of the plant system used. The influence and extent these factors need to be thoroughly investigated. Many studies have shown that nature has put in place various tolerance mechanisms to deal with these disturbances including antioxidant defense mechanisms involving elevated activities of enzymatic antioxidants such as super oxide dismutase (SOD) that either balance out or remove metals, as well as non-enzymatic antioxidants such as anthocyanins and carotenoids. DNA

Table 6. Chromosomal aberrations scored from Allium test

Treatments	Concentration	Duration	Chrm. Bridge	Lagging chrm.	Binucleate cells	Disturbed metaphase
Control			67.00 ± 3.00^{ab}	54.00 ± 2.00^{b}	60.00 ± 3.00^{b}	-
C. dolichopetalum AgNPs	0.5 mg	24h	-	-	51.00 ± 3.00^{c}	-
		48h	-	-	-	-
	1.0 mg	24h	-	-	-	-
		48h	-	-	-	-
C. bauchiense AgNPs	0.5 mg	24h	-	-	-	-
		48h	-	-	-	-
	1.0 mg	24h	-	-	-	-
		48h	-	-	-	-
C. racemosum AgNPs	0.5 mg	24h	-	-	-	-
		48h	-	-	-	-
	1.0 mg	24h	63.00 ± 6.00^{b}	-	-	-
		48h	-	-	-	-
C. platypterum AgNPs	0.5 mg	24h	-	-	-	-
		48h	-	-	-	-
	1.0 mg	24h	-	-	-	-
		48h	-	51.00 ± 1.00^{c}	-	52.00 ± 1.00^{a}
C. demeusei AgNPs	0.5 mg	24h	-	-	-	-
		48h	-	-	-	-
	1.0 mg	24h	-	-	-	-
		48h	-	-	-	-
C. paniculatum AgNPs	0.5 mg	24h	71.00 ± 4.00^{a}	-	-	-
		48h	-	-	63.00±2.00^{b}	-
	1.0 mg	24h	-	43.00 ± 1.00^{d}	-	-
		48h	-	57.00 ± 0.00^{a}	72.00 ± 7.00^{a}	-

Data are presented with means ± SE. Significant means were separated with different superscript alphabets along each column using Duncan New Multiple Range Test (DNMRT) at P < 0.05

repair mechanisms also take part by up regulation of genes associated with metal and oxidative stress responses (52).

Conclusion

All of the studied *Combretum* species demonstrated the ability to synthesize AgNPs, and the synthesized AgNPs exhibited similar results. XRD analysis revealed that the crystalline AgNPs exhibited 2 theta values in the 40° range, corresponding to miller indices of (200). Quantitative phytochemical screening indicated that flavonoids and phenolics had the highest concentration among the studied plants compared to other phytochemicals. The PDI values obtained from DLS fell within the standard range for stable nanoparticles, ranging from 0.3 – 0.6. Across all the study plants, the most prevalent functional groups were amide, amine, OH-hydroxyl and alkenes. The synthesized AgNPs displayed varying but significant antimicrobial activity, showing a trend towards a dose-dependent manner. In species where antimicrobial activity was minimal, higher concentrations of the AgNPs exhibited observable activities. The study introduced the nanoparticle production index (NPPI), the first of its kind and the findings suggested that smaller nanoparticles sizes correlates with higher production index, while larger sizes showed lower indices.

Acknowledgements

The authors would like to thank the Federal Government of Nigeria's Tertiary Education Trust Fund (TETFUND) for financial support.

Authors' contributions

SN and OS conceptualized and designed the study, and also drafted the manuscript. SN and CK conducted the research. UC performed statistical analysis, and also prepared the figures and tables. EG, CC and OE participated in the design, coordination of the research, and also helped draft the manuscript. All authors read and approved the final manuscript.

Compliance with ethical standards

Conflict of interest: Authors do not have any conflict of interest to declare.

Ethical issues: None .

References

1. Khan I, Saheed K, Khan I. Nanoparticles: Properties, applications and toxicities. Arab. J. Chem. 2019;12:908–931. https://doi.org/10.1016/j.arabjc.2017.05.011
2. Tan C, Cao X, Wu X, He Q, Yang J, Zhang X, Chen J, et al. Recent advances in ultrathin two-dimensional nanomaterials. Chem. Rev. 2017;117:6225–6331. https://doi.org/10.1021/acs.chemrev.6b00558
3. Zhang X, Liu Z, Shen W, Gurunathan S. Silver nanoparticles: Synthesis, characterization, properties, applications and therapeutic approaches. Int. J. Mol. Sci. 2016;17:1501–1534. https://doi.org/10.3390/ijms17091534
4. Dhanalakshmi T, Rajendran S. Synthesis of silver nanoparticles using *Tridax procumbens* and its antimicrobial activity. Arch. Appl. Sci. Res. 2012;4:12891–293.
5. Cale DF, Jessica S, Maria RP. Heterogeneous responses of ovarian cancer cells to silver nanoparticles as a single agent and in combination with cisplatin. J. Nanomater. 2017:11–1. https://doi.org/10.1155/2017/5107485
6. Carocho M, Ferreira ICFR. A review on antioxidants, prooxidants and related controversy: Natural and synthetic compounds, screening and analysis methodologies and future perspectives. Food Chem. Toxicol. 2013;51;15–25. https://doi.org/10.1016/j.fct.2012.09.021
7. Chahardoli A, Karimia N, Fattahi A. Biosynthesis, characterization, antimicrobial and cytotoxic effects of silver nanoparticles using *Nigella arvensis* seed extract. Iran. J. Pharm. Res. 2017;16:1167–1175. https://doi.org/10.22037/ijpr.2017.2066
8. Su H, Li S, Jin Y, Xian ZY, Yang D, Zhou W, et al. Nanomaterial-based biosensors for biological detections. Adv. Healthc. Technol. 2017;3:19–29. https://doi.org/10.2147/AHCT.S94025
9. Entsar HT, Noha MA. Effect of silver nanoparticles on the mortality pathogenicity and reproductivity of entomopathogenic nematodes. Int. J. Zool. Res. 2016;12:47–50. https://doi.org/10.3923/ijzr.2016.47.50
10. Borase HP, Salunkhe BK, Salunke RB, Patil CD, Hallsworth JE, Kim BS and Patil SV. Plant extract: A promising biomatrix for ecofriendly, controlled synthesis of silver nanoparticles. Biotechnol. Appl. Biochem. 2014;173:1–29. https://doi.org/10.1007/s12010-014-0831-4
11. Borase HP, Salunkhe RB, Patil CD, Suryawanshi RK, Salunke BK, Wagh ND, Patil SV. Innovative approach for urease inhibition by *Ficus carica* extract-fabricated silver nanoparticles: An *in vitro* study. Biotechnol. Appl. Biochem. 2015;62:780–784. https://doi.org/10.1002/bab.1341
12. Parveen K, Banse V, Ledwani L. Green synthesis of nanoparticles: Their advantages and disadvantages. In: *AIP Conference Proceedings*, AIP Publishing Centre, New York1724(1):id.02004. Available at www. http://adsabs.harvard.edu/abs/2016AIPC.1724b0048P. 2014.
13. Dawadi S, Katuwal S, Gupta A, Lamichhane U, Thapa R, Jaisi S, Parajuli N. Current research on silver nanoparticles: Synthesis, characterization, and applications. J. Nanomater. 2021;6:3–23. https://doi.org/10.1155/2021/6687290
14. Supraja S, Ali SM, Chakravarthy N, Jaya Prakash Priya A, Sagadevan E, Kasinathan MK, Arumugam P. Green synthesis of silver nanoparticles from *Cynodon dactylon* leaf extract. Int J Chem Tech Res. 2013;5:271–277.
15. Association of Official Analytical Chemists (AOAC). Official Methods of Analysis of AOAC International, 18th edition, Horwitz. W, Lalimer G, editors. Maryland-USA, Association of Official Analytical Chemists International, 2005. -96pp.
16. Kora AJ, Sashidhar RB, Arunachalam J. Gum kondagogu (*Cochlospermum gossypium*): A template for the green synthesis and stabilization of silver nanoparticles with antibacterial application. Carbohydr. Polym. 2010;82:670–679. https://doi.org/10.1016/j.carbpol.2010.05.034
17. Al-Ahmadi MS. Cytogenetic and molecular assessment of some nanoparticles using Allium sativum assay. Afr. J. Biotechnol. 2019;18:783–796. https://doi.org/10.5897/AJB2019.16918
18. Ibrahim HMM. Green synthesis and characterization of silver nanoparticles using banana peel extract and their antimicrobial activity against representative microorganisms. J. Radiat. Res. Appl. Sci. 2015;8:265–275. https://doi.org/10.1016/j.jrras.2015.01.007
19. Chahardoli A, Karimia N, Fattahi A. Biosynthesis, characterization, antimicrobial and cytotoxic effects of silver

nanoparticles using *Nigella arvensis* seed extract. Iran. J. Pharm. Res. 2017;16:1167–1175. https://doi.org/10.22037/ijpr.2017.2066

20. Chung I, Park I, Seung-Hyun K, Thiruvengadam M, Rajakumar G. Plant-mediated synthesis of silver nanoparticles: Their characteristic properties and therapeutic applications. Nanoscale Res. Lett. 2016;11(40):1–14. https://doi.org/10.1186/s11671-016-1257-4

21. Elumalai D, Hemavathi M, Deepa CV, Kaleena PK. Evaluation of phytosynthesized silver nanoparticles from leaf extracts of *Leucas aspera* and *Hyptis suaveolens* and their larvicidal activity against malaria, dengue and filariasis vectors. Parasite Epidemiol. Control. 2012;2:15–26. https://doi.org/10.1016/j.parepi.2017.09.001

22. Ghosh S, Patil S, Ahire, M., Kitture R, Kale S, Pardesi K, et al. Synthesis of silver nanoparticles using *Dioscorea bulbifera* tuber extract and evaluation of its synergistic potential in combination with antimicrobial agents. Int J Nanomedicine. 2012;27:483–496. https://doi.org/10.2147/IJN.S24793

23. Mikhailov OV, Mikhailova EO. Elemental silver nanoparticles: Biosynthesis and bio applications. Mater. 2019;12(19):3177–3210.https://doi.org/10.3390/ma12193177

24. Tak YK, Pal S, Naoghare PK, Rangasamy S, Song JM. Shape-dependent skin penetration of silver nanoparticles: Does it really matter?. Sci. Rep. 2015;5:16908–16911. https://doi.org/10.1038/srep16908

25. Ahmed S, Ikram S. Silver nanoparticles; one pot green synthesis using *Terminalia arjuna* extract for biological application. J Nanomed. Nanotechnol. 2015;6(4):1–6.

26. El-Rafie MH, Hamed AM. Antioxidant and anti-inflammatory activities of silver nanoparticles biosynthesized from aqueous leaf extracts of four *Terminalia* species. Adv. Nat. Sci.: Nanosci. Nanotechnol. 2014;5(3):1–11. https://doi.org/10.1088/2043-6262/5/3/035008

27. Ganesh B, Thulukkanan K, Amirthalingam T. Herbal nanosilver synthesized from *Terminalia paniculata* (Combretaceae) by green chemistry approach and testing its antimicrobial efficacy against human pathogen. Indian J. Sci. 2015;15(46):59–68.

28. Kumar MK, Sinha M, Mandal KB, Ghosh RA, Kumar SK,. Reddy SP. Green synthesis of silver nanoparticles using *Terminalia chebula* extract at room temperature and their antimicrobial studies. Spectrochim Acta A: Mol Biomol Spectrosc. 2012;91:228–233. https://doi.org/10.1016/j.saa.2012.02.001

29. Shah W, Patil U, Sharma A. Green synthesis of silver nanoparticles from stem bark extract of *Terminalia tomentosa* Roxb. (Wight and Arn.). Der Pharma Chem. 2014;6 (5):197–202.

30. Dada AO, Adekola FA, Adeyemi OS, Bello OM, Oluwaseun AC, Awakan OJ, Grace F A A. Exploring the effect of operational factors and characterization imperative to the synthesis of silver nanoparticles. In: Maaz K, editor. Silver Nanoparticles - Fabrication, Characterization and Applications. IntechOpen, London, UK. 2018. p. 165–184. https://doi.org/10.5772/intechopen.76947

31. Jyoti K, Baunthiyal M, Singh A. Characterization of silver nanoparticles synthesized using *Urtica dioica* Linn. leaves and their synergistic effects with antibiotics. J. Radiat. Res. Appl. Sci. 2016;9:217–227. https://doi.org/10.1016/j.jrras.2015.10.002

32. Anandalakshmi K, Venugobal J, Ramasamy V. - Characterization of silver nanoparticles by green synthesis method using *Pedalium murex* leaf extract and their antibacterial activity. Appl. Nanosci. 2016;6:399–408. https://doi.org/10.1007/s13204-015-0449-z

33. Christensen L, Vivekanandhan S, Misra M, Mohanty AK. Biosynthesis of silver nanoparticles using *Murraya koenigii* (curry leaf): An investigation on the effect of broth concentration in reduction mechanism and particle size. Adv. Mater. Lett. 2012;2:429–434. https://doi.org/10.5185/amlett.2011.4256

34. Nanocomposix. UV/VIS/IR Spectroscopy Analysis of Nanoparticles. 2012. http://50.87.149.212/sites/default/files/nanoComposix%20Guidelines%20for%20UVvis%0Analysis.pdf .

35. Bera B. Nanoporous silicon prepared by vapour phase strain etch and sacrificial technique. In: Proceedings of the International Conference on Microelectronic Circuit and System. (Kolkata, India). 2015. p. 42–45.

36. Nobbmann UL. Polydispersity – What does it mean for DLS and chromatography. 2014. http://www.materials-talks.com/blog/2014/10/23/polydispersity-what-does-it-mean-for-dls-and-chromatography/.

37. Jemal K, Sandeep BV, Pola S. Synthesis, characterization and evaluation of the antibacterial activity of *Allophylus serratus* leaf and leaf derived callus extract mediated silver nanoparticles. J. Nanomater. 2017;4:1–11. https://doi.org/10.1155/2017/4213275

38. Yan JK, Cai PF, Cao XQ, Ma HL, Zhang Q, Hu NZ, Zhao YZ. Green synthesis of silver nanoparticles using 4-acetamido-TEMPO-oxidized curdlan. Carbohydr. Polym. 2013;97: 391–397. https://doi.org/10.1016/j.carbpol.2013.05.049

39. Hussain M, Raja IN, Iqbal M, Aslam S. Applications of plant flavonoids in the green synthesis of colloidal silver nanoparticles and impacts on human health. Iran. J. Sci. Technol. Trans. A Sci. 2017;43(6):1–11. https://doi.org/10.1007/s40995-017-0431-6

40. Jain S, Mehata SM. Medicinal plant leaf extract and pure flavonoid mediated green synthesis of silver nanoparticles and their enhanced antibacterial property. Sci. Rep. 2017;7 (1):15867–15880. https://doi.org/10.1038/s41598-017-15724-8

41. Dawe A, Pierre S, Tsala ED, Habtemariam S. Phytochemical constituents of *Combretum* Loefl. (Combretaceae). Pharm. Crop. 2013;4:385–9. https://doi.org/10.2174/2210290601304010038

42. Niass O, Diop A, Mariko M, Géye R, Thiam, K, Sarr OS, Ndiaye, et al. Comparative study of the composition of aqueous extracts of green tea (*Camellia sinensis*) in total alkaloids, total flavonoids, total polyphenols and antioxidant activity with the leaves of *Combretum glutinosum*, *Combretum micranthum* and the red pulps of *Hibiscus sabdariffa*. Int. J. Progress. Sci. Technol. 2017;5:71–75.

43. Nounagon MS, Dah-Nouvlessounon D, N'tcha C, Akorede SM, Sina H. Phytochemical screening and biological activities of *Combretum adenogonium* leaves extracts. Eur. Sci. J. 2017;13:358–375. https://doi.org/10.19044/esj.2017.v13n30p358

44. Masum MI, Siddiqa M, Ali K, Zhang Y, Abdallah Y, Ibrahim E, et al. Biogenic synthesis of silver nanoparticles using *Phyllanthus emblica* fruit extract and its inhibitory action against the pathogen *Acidovorax oryzae* strain RS-2 of rice bacterial brown stripe. Front. Microbiol. 2019;10(820):1–18. https://doi.org/10.3389/fmicb.2019.00820

45. Sharma G, Nam JS, Sharma AR, Lee SS. Antimicrobial potential of silver nanoparticles synthesized using medicinal herb *Coptidis rhizome*. Mol. 2018;23(9):2268–2280. https://doi.org/10.3390/molecules23092268

46. Shehzad A, Qureshi M, Jabeen S, Ahmad R, Alabdalall AH, Aljafary MA, Al-Suhaimi E. Synthesis, characterization and antibacterial activity of silver nanoparticles using *Rhazya stricta*. PeerJ. 2018;6:e6086–e6101. https://doi.org/10.7717/

peerj.6086

47. Riss TL, Moravec RA, Niles AL. Cytotoxicity testing: Measuring viable cells, dead cells and detecting mechanism of cell death. Methods Mol. Biol. 2011;740:103–114. https://doi.org/10.1007/978-1-61779-108-6_12

48. Turkoglu S. Determination of genotoxic effects of chlorfenvinphos and fenbuconazole in *Allium cepa* root cells by mitotic activity, chromosome aberration, DNA content, and comet assay. Pestic. Biochem. Phys. 2012;103:224–230. https://doi.org/10.1016/j.pestbp.2012.06.001

49. Andrade LF, Davide LC, Gedraite LS. The effect of cyanide compounds, fluorides and inorganic oxides present in spent pot Liner on germination and root tip cells of *Lactuca sativa*. Ecotoxicol. Environ. Saf. 2010;73:626–631. https://doi.org/10.1016/j.ecoenv.2009.12.012

50. Wong C, Stearns T. Mammalian cells lack checkpoints for tetraploidy, aberrant centrosome number, and cytokinesis failure. BMC Cell Biol. 2005;6:1–12. https://doi.org/10.1186/1471-2121-6-6

51. Sarkar D, Sharma A, Talukder G. Plant extracts as modulators of genotoxic effects, Bronx, -NY, USA, Scientific Publications Department, The New York Botanical Garden, 1996. p. 276–300. https://doi.org/10.1007/BF02856614

52. Ma C, White JC, Dhankher OP, Xing B. Metal-based nanotoxicity and detoxification pathways in higher plants. Environ. Sci. Technol. 2015;49:7109–7122. https://doi.org/10.1021/acs.est.5b00685